

MODELING SEQUENCES WITH QUANTUM STATES: A LOOK UNDER THE HOOD

TAI-DANAE BRADLEY, MILES STOUDENMIRE, AND JOHN TERILLA

ABSTRACT. Classical probability distributions on sets of sequences can be modeled using quantum states. Here, we do so with a quantum state that is pure and entangled. Because it is entangled, the reduced densities that describe subsystems also carry information about the complementary subsystem. This is in contrast to the classical marginal distributions on a subsystem in which information about the complementary system has been integrated out and lost. A training algorithm based on the density matrix renormalization group (DMRG) procedure uses the extra information contained in the reduced densities and organizes it into a tensor network model. An understanding of the extra information contained in the reduced densities allow us to examine the mechanics of this DMRG algorithm and study the generalization error of the resulting model. As an illustration, we work with the even-parity dataset and produce an estimate for the generalization error as a function of the fraction of the dataset used in training.

CONTENTS

1. Introduction	2
Acknowledgments	3
2. Densities and reduced densities	3
2.1. Reconstructing a pure state from its reduced densities	5
3. Reduced densities of classical probability distributions	6
3.1. Learning from samples	9
4. The Training Algorithm	11
5. Under the hood	16
5.1. High-level summary	20
5.2. Combinatorics of reduced densities	22
6. Experiments	24
7. Conclusion	25
References	26

1. INTRODUCTION

In this paper, we present a deterministic algorithm for unsupervised generative modeling on strings using tensor networks. The algorithm is deterministic with a fixed number of steps and the resulting model has a perfect sampling algorithm that allows efficient sampling from marginal distributions, or sampling conditioned on a substring. The algorithm is inspired by the density matrix renormalization group (DMRG) procedure [1, 2, 3]. This approach, at its heart, involves only simple linear algebra which allows us to give a detailed “under the hood” look at the algorithm in action. Our analysis illustrates how to interpret the trained model and how to go beyond worst case bounds on generalization errors. We work through the algorithm with an exemplar dataset to produce a prediction for the generalization error as a function of the fraction used in training which well approximates the generalization error observed in experiments.

The machine learning problem of interest is to learn a probability distribution on a set of sequences from a finite training set of samples. For us, an important technical and conceptual first step is to pass from *Finite Sets* to *Functions on Finite Sets*. Functions on sets have more structure than sets themselves and we find that the extra structure is meaningful. Furthermore, well-understood concepts and techniques in quantum physics give us powerful tools to exploit this extra structure without incurring significant algorithmic costs [4]. We emphasize that it is not necessary that the datasets being modeled have any inherently quantum properties or interpretation. The inductive bias of the model can be understood as a kind of low-rank factorization hypothesis—a point we expand upon in this paper.

Reduced density operators play a central role in our model. In a happy coincidence, they play the central role in both the model’s theoretical inspiration and the training algorithm. There is structure in reduced densities that inspire us to model classical probability distributions using a quantum model. The training algorithm amounts to successively matching reduced densities, a process which leads inevitably to a tensor network model, which may be thought of as a sequence of compatible autoencoders. We refer readers unfamiliar with tensor diagram notation to references such as [5, 6, 7].

This paper also builds on investigations of tensor networks as models for machine learning tasks. Tensor networks have been demonstrated to give good results for supervised learning and regression tasks [8, 3, 9, 10, 11, 12, 13, 14]. They have also been applied successfully to unsupervised, generative modeling [15, 16, 17, 18] including a study based on the parity dataset we use here [17]. This work focuses on the latter task, proposing and studying an alternative algorithm for optimizing MPS for generative modeling. The expressivity of models like the one considered in this paper have been studied [19]. In this paper, we focus on understanding how our training algorithm learns to generalize.

Acknowledgments. The authors thank Gabriel Drummond-Cole, Glen Evenbly, James Stokes, and Yiannis Vlassopoulos for helpful discussions, and are happy to acknowledge KITP Santa Barbara, the Flatiron Institute, and Tunnel for support and excellent working conditions.

2. DENSITIES AND REDUCED DENSITIES

For our purposes, the passage from classical to quantum can be thought of as the passage from *Finite Sets* to *Functions on Finite Sets*, which have a natural Hilbert space structure. We are interested in probability distributions on finite sets. The quantum version of a probability distribution is a density operator on a Hilbert space. The quantum version of a marginal probability distribution is a reduced density operator. The operation that plays the role of marginalization is the partial trace. In our setup, the reduced densities contain more information than the marginal distributions associated to them and much of our work concerns this extra information.

Given a finite set S , one has the free vector space $V = \mathbb{C}^S$ consisting of complex valued functions on S , which is a Hilbert space with inner product

$$\langle f|g \rangle = \sum_{s \in S} \overline{f(s)}g(s).$$

The free vector space comes with a natural map from $S \rightarrow \mathbb{C}^S$, which we recall in a moment. To avoid confusion, it is helpful to use notation to distinguish between an element $s \in S$ and its image in \mathbb{C}^S , which is a vector. Commonly, the vector image of s is denoted with a boldface font or an overset arrow. We like the bra and ket notation, which is better when inner products are involved. For any $s \in S$, let $|s\rangle$ denote the function $S \rightarrow \mathbb{C}$ that sends $s \mapsto 1$ and $s' \mapsto 0$ for $s' \neq s$. The set $\{|s\rangle\}$ is an independent, orthonormal spanning set for V . If one chooses an ordering on the set S , say $S = \{s_1, \dots, s_d\}$, then $|s_j\rangle$ is identified with the j -th standard basis vector in \mathbb{C}^d , thus defining an isometric isomorphism of $V \xrightarrow{\sim} \mathbb{C}^d$ and a “one-hot” encoding $S \hookrightarrow \mathbb{C}^d$. More generally, we denote elements in V by ket notation $|\psi\rangle \in V$.

For any $|\psi\rangle \in V$, there is a linear functional in V^* whose value on $|\phi\rangle \in V$ is the inner product $\langle \psi|\phi \rangle$. We denote this linear functional by the succinct bra notation $\langle \psi| \in V^*$. Every linear functional in V^* is of the form $\langle \psi|$ for some $|\psi\rangle \in V$. We have vectors $|\psi\rangle \in V$ and covectors $\langle \psi| \in V^*$ and the map

$$|\psi\rangle \longleftrightarrow \langle \psi|$$

defines a natural isomorphism between V and V^* . We have chosen to distinguish between vectors and covectors with bra and ket notation; we will not imbue upper and lower indices with any special meaning.

When several spaces V, W, \dots are in play, some tensor product symbols are suppressed. So, for instance, if $|\psi\rangle \in V$ and $|\phi\rangle \in W$, we will write $|\psi\rangle|\phi\rangle$, or even $|\psi\phi\rangle$, instead of $|\psi\rangle \otimes |\phi\rangle \in V \otimes W$. An expression like $|\phi\rangle\langle \psi|$

is an element of $W \otimes V^*$, naturally identified with an operator $V \rightarrow W$. The expression $|\psi\rangle\langle\psi|$ is an element in $\text{End}(V)$. Here, $\text{End}(V)$ denotes the space of all linear operators on V and in the presence of a basis is identified with $\dim(V) \times \dim(V)$ matrices. If $|\psi\rangle$ is a unit vector, then the operator $|\psi\rangle\langle\psi|$ is orthogonal projection onto $|\psi\rangle$: it maps $|\psi\rangle \mapsto |\psi\rangle$ and maps every vector perpendicular to $|\psi\rangle$ to zero.

A *density operator*, or just *density* for short, is a unit-trace, positive semi-definite linear operator on a Hilbert space. Sometimes a density is called a quantum *state*. If S is a finite set and $V = \mathbb{C}^S$, then a density $\rho : V \rightarrow V$ defines a probability distribution on S by defining the probability $\pi_\rho : S \rightarrow \mathbb{R}$ by the *Born rule*

$$(1) \quad \pi_\rho(s) = \langle s|\rho|s\rangle.$$

Going the other way, there are multiple ways to define a density $\rho : V \rightarrow V$ from a classical probability distribution π on S so that $\pi_\rho = \pi$. One way is as a diagonal operator: $\rho_{diag} := \sum_{s \in S} \pi(s)|s\rangle\langle s|$. Another way is to define

$$(2) \quad \rho_\pi = |\psi\rangle\langle\psi| \text{ where } |\psi\rangle := \sum_{s \in S} \sqrt{\pi(s)}|s\rangle.$$

There exist other densities that realize π via the Born rule, but think of the diagonal density and projection onto $|\psi\rangle$ as two extremes. The density ρ_π has minimal rank and ρ_{diag} has maximal rank. In the language of quantum mechanics, a state is *pure* if it has rank one and is *mixed* otherwise. The degree to which a state is mixed is measured by its von Neumann entropy, $-\text{tr}(\rho \ln(\rho))$, which ranges from zero in the case of ρ_π up to the Shannon entropy of the classical distribution π in the case of ρ_{diag} . In this paper, we always use the pure state $\rho := \rho_\pi$. To summarize, we associate to any probability distribution $\pi : S \rightarrow \mathbb{R}$ the density $\rho_\pi : V \rightarrow V$ defined by Equation (2), which has the property that $\pi_{\rho_\pi} = \pi$.

If a set S is a Cartesian product $S = A \times B$ then the Hilbert space \mathbb{C}^S decomposes as a tensor product $\mathbb{C}^S \cong \mathbb{C}^A \otimes \mathbb{C}^B$. In this case, a density $\rho : \mathbb{C}^A \otimes \mathbb{C}^B \rightarrow \mathbb{C}^A \otimes \mathbb{C}^B$ is the quantum version of a joint probability distribution $\pi : A \times B \rightarrow \mathbb{R}$. By an operation that is analogous to marginalization, ρ gives rise to two densities $\rho_A : \mathbb{C}^A \rightarrow \mathbb{C}^A$ and $\rho_B : \mathbb{C}^B \rightarrow \mathbb{C}^B$ which we refer to as *reduced densities*. We now describe this operation, which is called *partial trace*.

If X and Y are finite dimensional vector spaces, then $\text{End}(X \otimes Y)$ is isomorphic to $\text{End}(X) \otimes \text{End}(Y)$. Using this isomorphism, there are maps

$$\begin{array}{ccc} & \text{End}(X \otimes Y) & \\ \text{tr}_Y \swarrow & & \searrow \text{tr}_X \\ \text{End}(X) & & \text{End}(Y) \end{array}$$

defined by

$$\text{tr}_Y(f \otimes g) := f \text{tr}(g) \text{ and } \text{tr}_X(f \otimes g) := g \text{tr}(f)$$

for $f \in \text{End}(X)$ and $g \in \text{End}(Y)$. The maps tr_Y and tr_X are called *partial traces*. The partial trace preserves both trace and positive semi-definiteness and so the image of any density $\rho \in \text{End}(X \otimes Y)$ under partial trace defines *reduced densities* $\text{tr}_Y \rho \in \text{End}(X)$ and $\text{tr}_X \rho \in \text{End}(Y)$.

It is worth noting that while we have maps $\text{End}(X) \otimes \text{End}(Y) \rightarrow \text{End}(X)$ and $\text{End}(X) \otimes \text{End}(Y) \rightarrow \text{End}(Y)$, there do not exist natural maps $V \otimes W \rightarrow V$ or $V \otimes W \rightarrow W$ for arbitrary vector spaces V and W ; partial trace is special, it is defined in the case that V and W are endomorphism spaces.

2.1. Reconstructing a pure state from its reduced densities. We now discuss the problem of reconstructing a pure quantum state ρ on a product $X \otimes Y$ from its reduced densities ρ_X and ρ_Y .

Using the isomorphism $X \cong X^*$ that is available in any finite dimensional Hilbert space, one can view any vector $|\psi\rangle$ in a product of Hilbert spaces $X \otimes Y$ as an element of $X^* \otimes Y$, hence as a linear map $M: X \rightarrow Y$. Computationally, if $|\psi\rangle$ is expressed using bases $\{|a\rangle\}$ of X and $\{|b\rangle\}$ of Y as

$$|\psi\rangle = \sum_{a,b} m_{ab} |a\rangle \otimes |b\rangle$$

then the coefficients $\{m_{ab}\}$ of that sum can be reshaped into a $\dim(Y) \times \dim(X)$ matrix M . A singular value decomposition (SVD) of M gives a factorization $M = VDU^*$ with V and U unitary and D diagonal as in Figure 1.

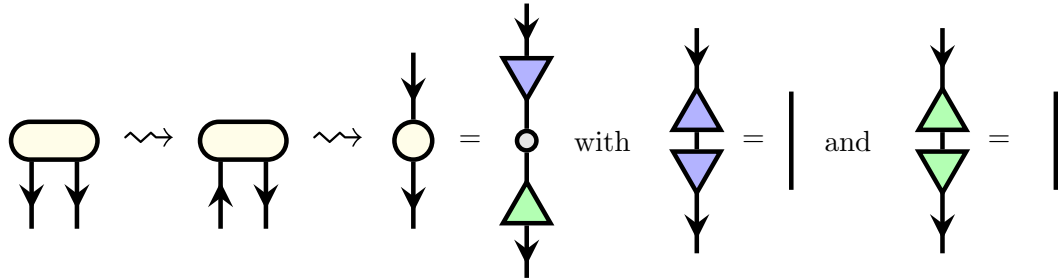


FIGURE 1. A tensor network diagram following $|\psi\rangle \in X \otimes Y$ through the isomorphisms $X \otimes Y \cong X^* \otimes Y \cong \text{hom}(X, Y)$, leading to the singular value decomposition of $M = VDU^*$ with the unitarity of V and U .

The columns $\{|f_i\rangle\}$ of the matrix V are the left singular vectors of M . They are the eigenvectors of MM^* and comprise an orthonormal basis for the image of M . The columns $\{|e_i\rangle\}$ of the matrix of U are the right singular vectors of M . They are the eigenvectors of M^*M , an orthonormal set of vectors spanning a subspace of X isomorphic to the image of M . The nonnegative real numbers $\{\sigma_i\}$ on the diagonal of D are the singular values

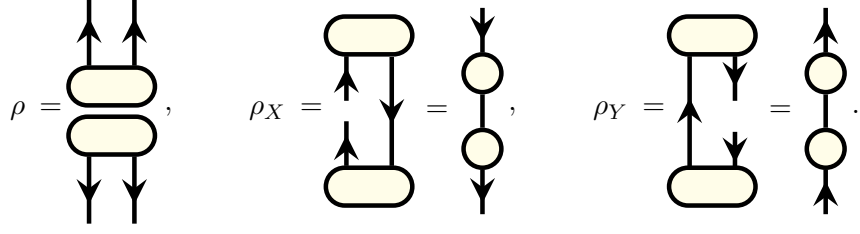


FIGURE 2. A tensor network diagram showing that $\rho_X = M^*M$ and $\rho_Y = MM^*$.

of the matrix M . The matrices M^*M and MM^* have the same eigenvalues $\{\lambda_i\}$ which are the squares of the singular values $\lambda_i := |\sigma_i|^2$. The map M defines a bijection between the $\{|e_i\rangle\}$ and $\{|f_i\rangle\}$. Specifically, M acts as

$$(3) \quad |e_i\rangle \mapsto \sigma_i |f_i\rangle$$

and maps the perpendicular complement of the span of the $\{|e_i\rangle\}$ to zero.

Now, given a unit vector $|\psi\rangle \in X \otimes Y$, we have the density $\rho = |\psi\rangle\langle\psi| \in X \otimes Y \otimes Y^* \otimes X^*$ and the reduced densities $\rho_X : X \rightarrow X$ and $\rho_Y : Y \rightarrow Y$. The reduced densities of ρ are related to the operator $M : X \rightarrow Y$ fashioned from $|\psi\rangle$ as follows

$$(4) \quad \rho_X = M^*M \text{ and } \rho_Y = MM^*$$

as illustrated in Figure 2. The singular vectors $\{|e_i\rangle\}$ and $\{|f_i\rangle\}$ of M are precisely the eigenvectors of the reduced densities. Therefore, the density ρ can be completely reconstructed from its reduced densities ρ_X and ρ_Y . One obtains $|\psi\rangle$ by gluing the eigenvectors of the reduced densities along their shared eigenvalues (Figure 3). In the nondegenerate case that the eigenvalues are distinct, then there is a unique way to glue the $\{|e_i\rangle\}$ and the $\{|f_i\rangle\}$ and $|\psi\rangle$ is recovered perfectly.

3. REDUCED DENSITIES OF CLASSICAL PROBABILITY DISTRIBUTIONS

Let $\pi : S \rightarrow \mathbb{R}$ be a probability distribution and consider the density ρ_π as in Equation (2). Suppose $S \subset A \times B$ and let $\rho_A = \text{tr}_Y \rho$ and $\rho_B = \text{tr}_X \rho$ denote the reduced densities where, as above, $X = \mathbb{C}^A$, $Y = \mathbb{C}^B$, and $V = X \otimes Y$. Let us now interpret the matrix representation of these reduced

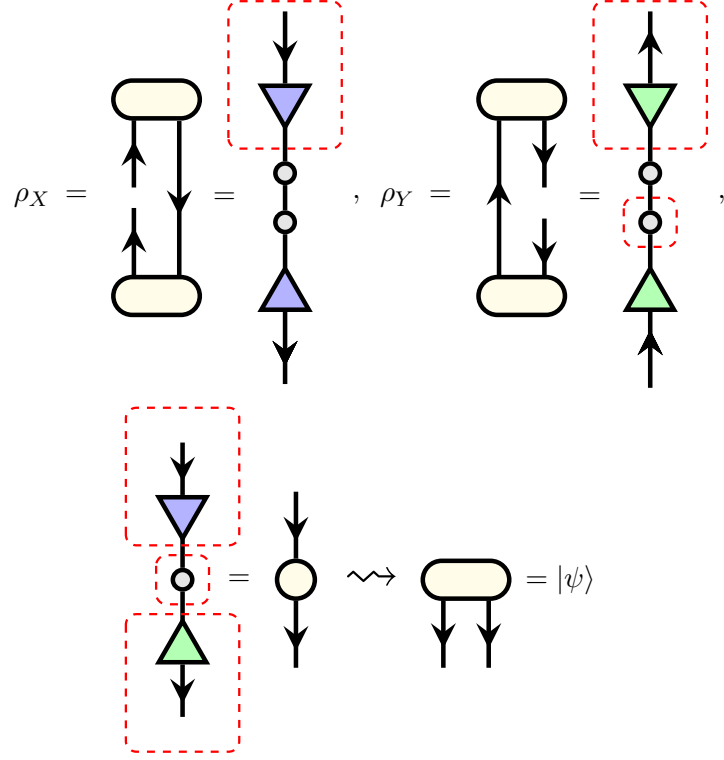


FIGURE 3. Reconstructing $|\psi\rangle$ from the eigenvectors of ρ_X and ρ_Y and their shared eigenvalues.

densities. We compute:

$$\begin{aligned}
 \rho &= |\psi\rangle\langle\psi| \\
 &= \left(\sum_{(a,b) \in S} \sqrt{\pi(a,b)} |a\rangle \otimes |b\rangle \right) \otimes \left(\sum_{(a',b') \in S} \sqrt{\pi(a',b')} \langle a'| \otimes \langle b'| \right) \\
 &= \sum_{\substack{(a,b) \in S \\ (a',b') \in S}} \sqrt{\pi(a,b)} \sqrt{\pi(a',b')} |a\rangle \langle a'| \otimes |b\rangle \langle b'|
 \end{aligned}$$

We compute the partial trace $\text{tr}_Y(|a\rangle\langle a'| \otimes |b\rangle\langle b'|) = \langle b|b'\rangle |a\rangle\langle a'|$. Since $\langle b|b'\rangle = 1$ if $b = b'$ and zero otherwise, we can understand the (a, a') entry of the reduced density ρ_A as

$$(5) \quad (\rho_A)_a^{a'} = \sum_{b \in B} \sqrt{\pi(a,b)\pi(a',b)}.$$

In particular, the diagonal entry $(\rho_A)_a^a$ is $\sum_{b \in B} \pi(a,b)$ and we see the marginal distribution $\pi_A : A \rightarrow \mathbb{R}$ along the diagonal of the reduced density ρ_A . We make the consistent observation that ρ_A has unit trace. The off-diagonal

entries of ρ_A are determined by the extent to which $a, a' \in A$ have the same continuations in B . Note that ρ_A is symmetric. The reduced density on B is similarly given:

$$(6) \quad (\rho_B)_b^{b'} = \sum_{a \in A} \sqrt{\pi(a, b)\pi(a, b')}.$$

So, the reduced densities of ρ contains all the information of the marginal distributions π_A and π_B and more. Now, let's take a look at the extra information carried by the reduced densities, which is entirely contained in the off diagonal entries. Since the entire state, and therefore π itself, can be reconstructed from the eigenvectors and eigenvalues of ρ_A and ρ_B , we know that from a high level this spectral information encodes the conditional probabilities that are lost by the classical process of marginalization. En route to decoding this spectral information, let us describe how an arbitrary density τ is a classical mixture model of pure quantum states. If $|e_1\rangle, \dots, |e_k\rangle$ is a basis for the image of a density τ consisting of orthonormal eigenvectors, then the corresponding eigenvalues $\lambda_1, \dots, \lambda_k$ are nonnegative real numbers whose sum is one. One has

$$\tau = \sum_{i=1}^k \lambda_i |e_i\rangle\langle e_i|$$

The density τ defines a probability distribution on pure states: the probability of the pure state $|e_i\rangle\langle e_i|$ being λ_i . Then, $|e_i\rangle\langle e_i|$ defines a probability distribution on the computational basis $\{s\}$ via the Born Rule: the probability of s is $\langle s|e_i\rangle\langle e_i|s\rangle = |\langle e_i|s\rangle|^2$.

We're interested in the reduced densities of $\rho = |\psi\rangle\langle\psi|$ and in this case there exists a one-to-one correspondence $|e_i\rangle \leftrightarrow |f_i\rangle$ between eigenvectors of the reduced densities $\rho_A := \text{tr}_Y(\rho)$ and $\rho_B := \text{tr}_X(\rho)$ spanning their respective images.

$$\rho_A = \sum_{i=1}^k \lambda_i |e_i\rangle\langle e_i| \text{ and } \rho_B = \sum_{i=1}^k \lambda_i |f_i\rangle\langle f_i|.$$

as outlined in Section 2.1.

Putting together the general picture of a density as a mixture of pure states with the reduced densities of a pure state leads one to the following paradigm. With probability λ_i the prefix subsystem will be in a state determined by the corresponding eigenvector $|e_i\rangle$ of ρ_A , and the corresponding suffix subsystem will be in a state determined by the eigenvector $|f_i\rangle$. The vector $|e_i\rangle = \sum_a \gamma_i^a |a\rangle$ determines a probability distribution on the set of prefixes A : the probability of the prefix a is $|\gamma_i^a|^2$. The vector $|f_i\rangle = \sum_b \beta_i^b |b\rangle$ determines a probability distribution on the set of suffixes B : the probability of b is $|\beta_i^b|^2$.

As a final remark, if we had begun with the diagonal density

$$\rho_{diag} = \sum_{(a,b) \in A \times B} \pi(a,b) (|a\rangle \otimes |b\rangle) \otimes (\langle b| \otimes \langle a|)$$

whose Born distribution is also π , then the matrices representing ρ_A and ρ_B would be diagonal matrices with marginal distributions on A and B along the diagonals and all off diagonal elements are zero. The eigenvectors of ρ_A and ρ_B are simply the prefixes $|a\rangle$ and suffixes $|b\rangle$ and carry no further information. The process of computing reduced densities of ρ_{diag} is nothing more than the process of marginalization. We always use the pure state $\rho = |\psi\rangle\langle\psi|$ ensuring that the reduced densities carry information about subsystem interactions. The eigenvectors of the reduced densities, which are linear combinations of prefixes and linear combinations of suffixes, interact through their eigenvalues and capture rich information about the prefix-suffix system.

Let us summarize. Begin with a classical probability distribution π on a product set $S = A \times B$. Form a density ρ_π on $\mathbb{C}^{A \times B}$ by the formula in Equation (2). The reduced densities ρ_A and ρ_B on \mathbb{C}^A and \mathbb{C}^B contain marginal distributions π_A and π_B on their diagonals, but they are not diagonal operators. The eigenvectors of these reduced densities encode information about prefix-suffix interactions. The prefix-suffix interactions are tantamount to conditional probabilities and carry sufficient information to reconstruct the density ρ .

3.1. Learning from samples. In the machine learning applications to come, the goal is to learn ρ_π defined in Equation (2) from a set $\{s_1, \dots, s_{N_T}\}$ of samples drawn from a probability distribution π . Each sample s_i will be a sequence (x_1, \dots, x_N) of a fixed length N . The algorithm to learn the density ρ_π on the full set of sequences S is an inductive procedure.

One only works with a density ρ defined using the sample set since the density ρ_π for the entire distribution π is unavailable. The procedure begins by computing the reduced density ρ_A and its eigenvectors for a subsystem A consisting of short prefixes. Step by step, the size of the subsystem A is increased until one reaches a point where the suffix subsystem B is small. In a final step, ρ is recombined from the collected eigenvectors of ρ_A for all the prefix systems A and the eigenvectors and eigenvalues of ρ_B . This procedure leads naturally to a tensor network approximation for ρ .

An important point is that the reduced density ρ_A operates in a space whose dimension grows exponentially with the length of the prefix system A . So, instead of computing ρ_A exactly, it is computed by a sequence of approximations that keep its rank small. The modeling hypothesis is that π is a distribution whose corresponding quantum state ρ_π has low rank in the sense that the reduced densities ρ_A and ρ_B are low rank operators for all prefix-suffix subsystems A and B . The large rank of the density ρ witnessed from the empirical distribution drawn from π is regarded as sampling error.

Therefore, under the modeling hypothesis, the process of replacing the empirically computed reduced densities with low rank approximations should be thought of as repairing a state damaged by sampling errors. The low rank modeling hypothesis can lead to excellent generalization properties for the model.

Let us continue our analysis of the reduced densities as in the previous sections using notation appropriate for the machine learning algorithm. Let T be a training set of labeled samples $T = \{s_1, \dots, s_{N_T}\}$. We use N_T for the number of training examples. Each sample s_i will be a sequence of symbols from a fixed alphabet Σ of a fixed length N . We will designate a cut to obtain a prefix a_i and suffix b_i whose concatenation is the sample $s_i = (a_i, b_i) \in \Sigma^N$. This provides a decomposition of T as $T \subset A \times B$ where $A = \{a_1, a_2, \dots, a_{N_T}\}$ and $B = \{b_1, b_2, \dots, b_{N_T}\}$ are the sampled prefixes and suffixes. For the applications we have in mind, samples in T will be distinct. That is $(a_i, b_i) \neq (a_j, b_j)$ if $i \neq j$, though crucially it may happen that $a_i = a_j$ or $b_i = b_j$ for $i \neq j$. Let $\hat{\pi}$ be the resulting empirical distribution on T so that

$$(7) \quad \hat{\pi}(a, b) = \begin{cases} 1/\sqrt{N_T} & \text{if } (a, b) \in T, \\ 0 & \text{otherwise.} \end{cases}$$

Let us look at the empirical state

$$(8) \quad |\psi\rangle = \frac{1}{\sqrt{N_T}} \sum_{i=1}^{N_T} |s_i\rangle,$$

the empirical density $\rho = |\psi\rangle\langle\psi|$, and its partial trace

$$(9) \quad \rho_A = \frac{1}{N_T} \sum_{i,j=1}^{N_T} s(a_i, a_j) |a_i\rangle\langle a_j|.$$

Here the sum is expressed in terms of the indices i, j , which range over the number of samples. The coefficient $s(a_i, a_j)$ of $|a_i\rangle\langle a_j|$ is a nonnegative integer, namely the number of times that a_i and a_j have the same continuation $b_i = b_j$. It may be convenient to have some notation for shared continuations. For any pair a, a' of elements of A , let $T_{a,a'}$ be the subset of B consisting of shared continuations of a and a' :

$$(10) \quad T_{a,a'} = \{b \in B : (a, b) \in T \text{ and } (a', b) \in T\}.$$

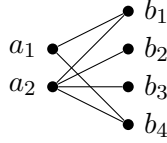
So, the (a, a') entry of the matrix representing ρ_A is the cardinality of the set $T_{a,a'}$ divided by an overall factor of $1/N_T$.

A similar combinatorial description holds for the reduced density on B ,

$$\rho_B = \frac{1}{N_T} \sum_{i,j} s(b_i, b_j) |b_i\rangle\langle b_j|$$

where $s(b_i, b_j)$ is the number of common prefixes that b_i and b_j share.

The counting involved can be visualized with graphs. Every probability distribution $\hat{\pi}$ on a Cartesian product $A \times B$ uniquely defines a weighted bipartite graph: the two vertex sets are A and B and the edge joining a and b is labeled by $\hat{\pi}(a, b)$. Here, because we assume the samples in T are distinct, the graph can be simplified since $\hat{\pi}(a, b)$ is either 0 or $1/N_T$. We draw an edge from a to b if $(a, b) \in T$ and we omit the edge if $(a, b) \notin T$ and understand the probabilities to be obtained by dividing by N_T , which is the total number of edges in the graph.



In the example above, the total number of edges is the sample size $N_T = 6$. The probability of $(a_1, b_1) = 1/6$ and the probability of $(a_1, b_2) = 0$. Now we illustrate how to read off the entries of the reduced density ρ_A from the graph. There will be an overall factor of $1/N_T$ multiplied by a matrix of nonnegative integers. The diagonal entries are $d(a)$, the degree of vertex a . The (a, a') entry is the number of shared suffixes, which equals the number of paths of length 2 between a and a' , divided by 6.

Given any graph with $|A| = 2$, such as the one above, the reduced density on the prefix subsystem is equal to

$$(11) \quad \rho_A = \frac{1}{N_T} \begin{bmatrix} d_1 & s \\ s & d_2 \end{bmatrix}$$

where the diagonal entries are the degrees of the vertices and s is the number of paths of length two, which equals the number of degree two vertices of B . The denominator of the coefficient $N_T = d_1 + d_2$ is the total number of edges in the graph. The eigenvalues λ_+ and λ_- and (unnormalized) eigenvectors e_+ and e_- of this matrix have simple, explicit expressions in terms of the gap $G = d_1 - d_2$ in the diagonal entries and the off-diagonal entry s . Namely,

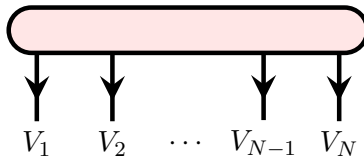
$$(12) \quad \lambda_+ = \frac{N_T + \sqrt{G^2 + 4s^2}}{2N_T} \text{ and } \lambda_- = \frac{N_T - \sqrt{G^2 + 4s^2}}{2N_T}$$

and

$$(13) \quad |e_+\rangle = \begin{bmatrix} \sqrt{G^2 + 4s^2} + G \\ +2s \end{bmatrix} \text{ and } |e_-\rangle = \begin{bmatrix} \sqrt{G^2 + 4s^2} - G \\ -2s \end{bmatrix}.$$

4. THE TRAINING ALGORITHM

Suppose that $|\psi\rangle \in V_1 \otimes \cdots \otimes V_N$. We depict $|\psi\rangle$ as



There are various sorts of decompositions of such a tensor that are akin to an iterated SVD. We will describe one decomposition that results in a factorization of $|\psi\rangle$ into what is called a matrix product state (MPS) or synonymously, a tensor train decomposition. The process defines a sequence of “bond” spaces $\{B_k\}$ and operators $\{U_k : B_k \otimes V_k \rightarrow B_{k-1}\}$ which can be composed $U_1 U_2 \cdots U_{N-1} U_N$ as pictured:

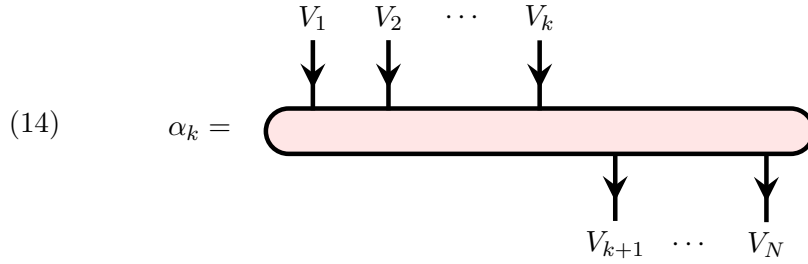


The initial operator has form $U_1 : B_1 \rightarrow V_1$ and the final tensor has the form $U_N \in B_{N-1} \otimes V_N$. We begin with $B_1 = V_1$ and set $U_1 : B_1 \rightarrow V_1$ to be the identity. For $k = 2, \dots, N-1$ we will define U_k inductively.

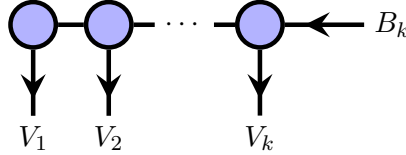
To describe the inductive process, first notice that for any $k = 1, \dots, N-1$, one has the tensor factorization

$$V_1 \otimes \cdots \otimes V_N \cong (V_1 \otimes \cdots \otimes V_k) \otimes (V_{k+1} \otimes \cdots \otimes V_N).$$

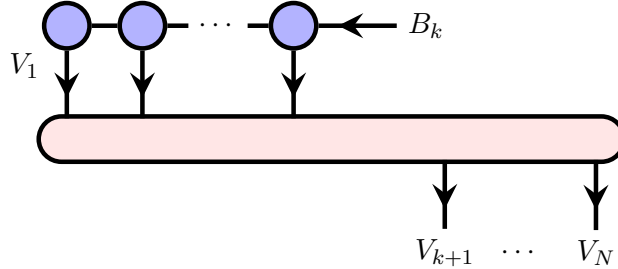
The operator $\alpha_k : V_1 \otimes \cdots \otimes V_k \rightarrow V_{k+1} \otimes \cdots \otimes V_N$ fashioned from $|\psi\rangle$ may be pictured as follows:



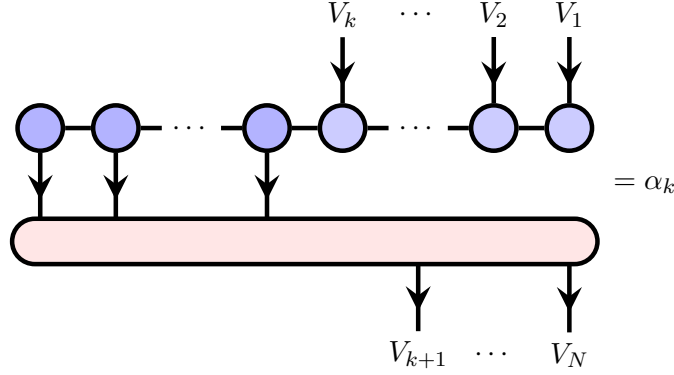
The operators U_k when composed $U_1 U_2 \cdots U_k$ as below



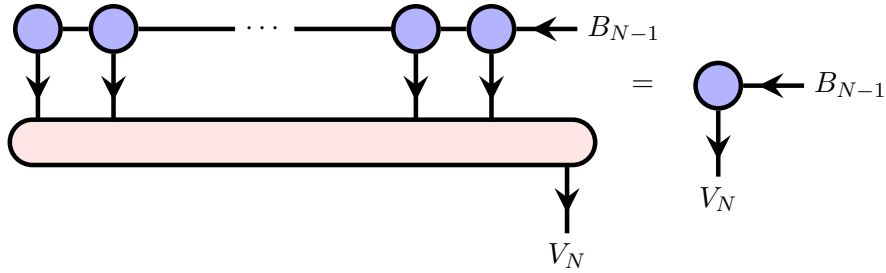
define an operator $B_k \rightarrow V_1 \otimes \cdots \otimes V_k$. One then has the composition $\beta_k := \alpha_k U_1 U_2 \cdots U_k : B_k \rightarrow V_{k+1} \otimes \cdots \otimes V_N$:



The inductive hypothesis is that $\alpha_k U_1 U_2 \cdots U_k U_k^* \cdots U_2^* U_1^* = \alpha_k$. Pictorially,



In the penultimate step, one has the operator $\alpha_{N-1} U_1 U_2 \cdots U_{N-1} : B_{N-1} \rightarrow V_N$. The final step is to define U_N as the adjoint of this operator: $U_N = (\alpha_{N-1} U_1 U_2 \cdots U_{N-1})^*$.



Therefore, the entire composition reduces nicely:

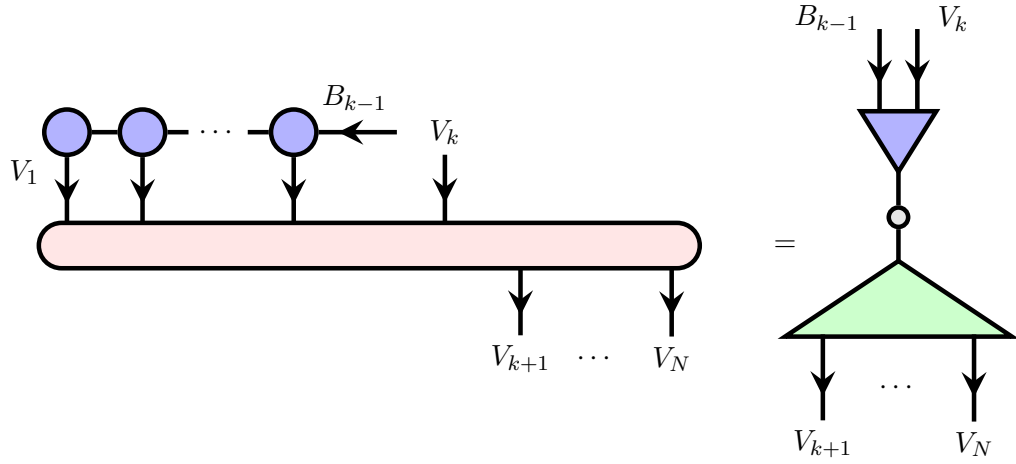
$$\begin{aligned} U_1 U_2 \cdots U_{N-1} U_N &= U_1 U_2 \cdots U_{N-1} U_{N-1}^* \cdots U_2^* U_1^* \alpha_{N-1}^* \\ &= \alpha_{N-1}^* \end{aligned}$$

The final equality follows from the adjoint of the inductive hypothesis. The outcome $\alpha_{N-1}^* : V_N^* \rightarrow V_1 \otimes \cdots \otimes V_{N-1}$, after a minor reshaping, is the same as $|\psi\rangle$.

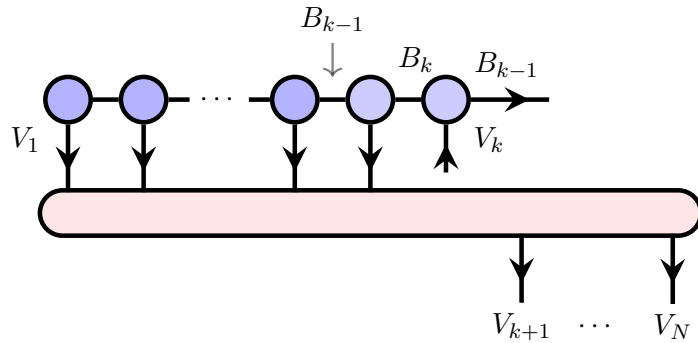
To define the inductive step, assume the spaces B_1, \dots, B_{k-1} and operators U_k have been defined and satisfy the inductive hypothesis. Reshape the operator $B_{k-1} \rightarrow V_k \otimes V_{k+1} \otimes \cdots \otimes V_N$ as a map

$$B_{k-1} \otimes V_k \rightarrow V_{k+1} \otimes \cdots \otimes V_N$$

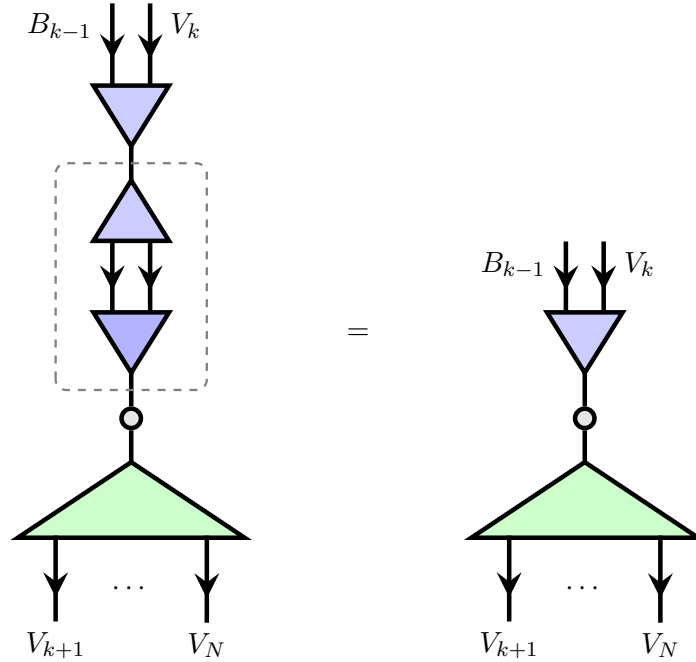
An SVD decomposition of this map yields $\alpha_{k-1} U_1 \cdots U_{k-1} = W_k D_k U_k^*$.



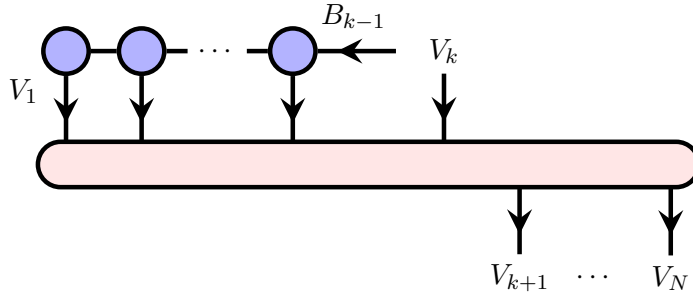
The adjoint of the map $U_k^* : B_{k-1} \otimes V_k \rightarrow B_k$, pictured as the blue triangle on the right hand side, is then defined to be $U_k : B_k \rightarrow B_{k-1} \otimes V_k$ and becomes the next tensor in the MPS decomposition. To check that the inductive hypothesis is satisfied, note that $\alpha_k U_1 \cdots U_{k-1} U_k U_k^* = \alpha_{k-1} U_1 \cdots U_{k-1}$ since $\alpha_{k-1} U_1 \cdots U_{k-1} = W_k D_k U_k^*$ and $U_k^* U_k = 1$. Here is the picture proof:



is equal to this



which is the first picture:

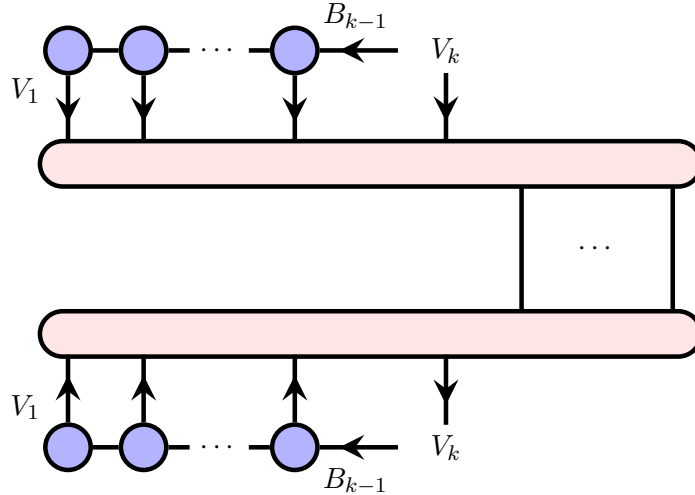


In our application, the vector $|\psi\rangle$ and the operators $\beta_{k-1} : B_{k-1} \otimes V_k \rightarrow V_{k+1} \otimes \cdots \otimes V_N$ operate in spaces of such high dimensions that neither they, nor a direct SVD of them, is feasible. Nonetheless, the U_k operators can be obtained from an SVD of a reduced density operating in the effective space $B_{k-1} \otimes V_k$

$$\beta_{k-1}^* \beta_{k-1} : B_{k-1} \otimes V_k \rightarrow B_{k-1} \otimes V_k$$

In our application, the effective reduced density $\beta_{k-1}^* \beta_{k-1}$ can be computed as a double sum over the training examples and we can efficiently compute the tensors required for the inductive steps. Then in the final step, the complementary space is small so the final map $U_N D_N : B_{N-1} \rightarrow V_N$ completes the reconstruction.

More specifically, to define the U_k , we only need an eigenvector decomposition of $\beta_{k-1}^* \beta_{k-1}$, which looks like



and is given by a formula like the one in Equation (9).

In general, when factoring an arbitrary vector as an MPS, the bond spaces B_k grow large exponentially fast. Therefore, we may characterize data sets for which the MPS model is a good model by saying that $|\psi\rangle$ as defined in Equation (2) has an MPS model whose bond spaces B_k remain small. Alternatively, one can truncate or restrict the dimensions of the spaces B_k resulting in a low rank MPS approximation of $|\psi\rangle$. As a criterion for this truncation, one can inspect the singular values at each inductive step and discard those which are small according to a pre-determined cutoff, and the corresponding columns of U and W . In the even-parity dataset that we investigate as an example, we always truncate B_k to two dimensions throughout.

To understand whether this kind of low-rank approximation is useful, remember that we understand that the eigenvectors and eigenvalues of the reduced densities carry the essential prefix-suffix interactions. By having a training algorithm that emphasizes these eigenvalues and eigenvectors as the most important features of the data throughout training, the resulting model should be interpreted as capturing the most important prefix-suffix interactions. We view these prefix-suffix interactions a proxy for the meaning of substrings within a language of larger strings.

5. UNDER THE HOOD

With an in-depth understanding of the training algorithm, we aim to predict experimental results, simply given the fraction $0 < f \leq 1$ of training samples used. Such an under-the-hood analysis shows that each tensor within the MPS is comprised of eigenvectors of a reduced density operator. The eigenvectors can be understood in terms of the reduced density matrix representation, which contains information from errors accrued in the algorithm's prior steps, along with combinatorial information from the current step. We now describe these ideas in careful detail.

As an example, we perform an analysis of how well the algorithm learns on the even-parity dataset. Let $\Sigma = \{0, 1\}$ and consider the set Σ^N of bitstrings of a fixed length N . Define the *parity* of a bitstring (b_1, \dots, b_N) to be

$$(15) \quad \text{parity}(b_1, \dots, b_N) := \sum_{i=1}^N b_i \pmod{2}.$$

The set Σ^N is partitioned into even and odd bitstrings:

$$E^N = \{s \in \Sigma^N : \text{parity}(s) = 0\} \text{ and } O^N = \{s \in \Sigma^N : \text{parity}(s) = 1\}$$

Consider the probability distribution $\pi : \Sigma^N \rightarrow \mathbb{R}$ uniformly concentrated on E^N :

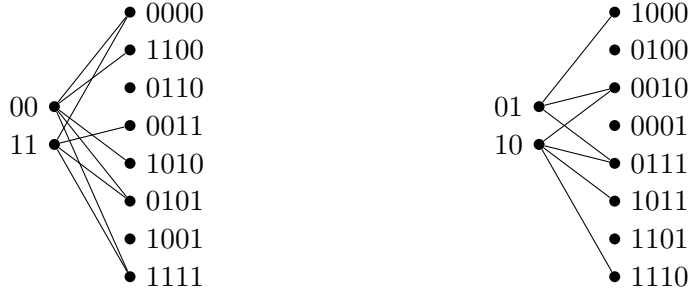
$$\pi(x) = \begin{cases} \frac{1}{2^{N-1}} & \text{if } x \in E^N \\ 0 & \text{if } x \in O^N. \end{cases}$$

This distribution defines a density $\rho_\pi = |E_N\rangle\langle E_N|$ where

$$(16) \quad |E_N\rangle = \frac{1}{\sqrt{2^{N-1}}} \sum_{s \in E^N} |s\rangle \in V_1 \otimes V_2 \otimes \dots \otimes V_N$$

where $V_j \cong \mathbb{C}^2$ is the site space spanned by the bits in the j -th position. Choose a subset $T = \{s_1, \dots, s_{N_T}\} \subset E_N$ of even parity bitstrings and let $f = N_T/2^{N-1}$ be the fraction selected. The empirical distribution on this set defines the vector $|\psi\rangle = \frac{1}{\sqrt{N_T}} \sum_{i=1}^{N_T} |s_i\rangle$ as in Equation (8). To begin our analysis on $|\psi\rangle$, let us closely inspect the algorithm's second step. The ideas therein will generalize to subsequent steps.

In step 2, we view each sample s as a prefix-suffix pair (a, b) where $a \in \Sigma^2$ and $b \in \Sigma^{N-2}$. We visualize the training set T as a bipartite graph. Vertices represent prefixes a and suffixes b and there is an edge joining a and b if and only if $(a, b) \in T$.



Notice that samples in the left graph are concatenations of even parity bitstrings; samples in the right graph are concatenations of odd parity bitstrings. Let $|\psi_2\rangle \in \mathbb{C}^{\Sigma^2} \otimes \mathbb{C}^{\Sigma^{N-2}}$ denote the sum of the samples after having completed step 1,

(17)

$|\psi_2\rangle =$

and consider the reduced density $\rho_2 = \text{tr}_{\Sigma^{N-2}} |\psi_2\rangle\langle\psi_2|$. The entries of its matrix representation are understood from the data in the graph. Choosing an ordering on the set Σ^2 , we write ρ_2 as

(18)

$$\rho_2 = \frac{1}{N_T} \begin{bmatrix} d_1 & s_e & 0 & 0 \\ s_e & d_2 & 0 & 0 \\ 0 & 0 & d_3 & s_o \\ 0 & 0 & s_o & d_4 \end{bmatrix}$$

The number of training samples N_T is the total number of edges in the graph. The diagonal entries are the degrees of vertices associated to prefixes: d_1 is the degree of 00, d_2 is the degree of 11, d_3 is the degree of 01, d_4 is the degree of 10. The off-diagonal entries are the number of paths of length 2 in each component of the graph. That is, s_e is the number of suffixes that 00 and 11 have in common; s_o is the number of suffixes that 01 and 10 have in common. If T contains all samples then both graphs are complete bipartite and the entries of ρ_2 are all equal (to 2^{N-3} in this case). In this case, ρ_2 is a rank 2 operator. It has two eigenvectors—one from each block. This is the idealized scenario: every sequence is present in the training set, the tensor obtained $\rho_2 = U_2 D_2 U_2^*$ is then

$$\rho_2 = \frac{1}{2} (|E_2\rangle\langle E_2| \oplus |O_2\rangle\langle O_2|)$$

where $|E_2\rangle = \frac{1}{\sqrt{2}}(|00\rangle + |11\rangle)$ denotes the normalized sum of even prefixes of length 2, and $|O_2\rangle = \frac{1}{\sqrt{2}}(|01\rangle + |10\rangle)$ denotes the normalized sum of odd prefixes of length 2. As a matrix, U_2 has $|E_2\rangle$ and $|O_2\rangle$ along its rows. We think of it as a “summarizer”: it projects a prefix onto an axis that can be identified with either $|E_2\rangle$ or $|O_2\rangle$ according to its parity, perfectly summarizing the information of that prefix required to understand which suffixes it is paired with.

More generally, however, if $T \neq E_N$ then the reduced density ρ_2 may be full rank. In this case we choose the eigenvectors $|E'_2\rangle, |O'_2\rangle$ that correspond to the two largest eigenvalues of ρ_2 . We assume these eigenvectors come from distinct blocks. This defines the tensor U_2 , which as a matrix has $|E'_2\rangle$ and $|O'_2\rangle$ along its rows, where

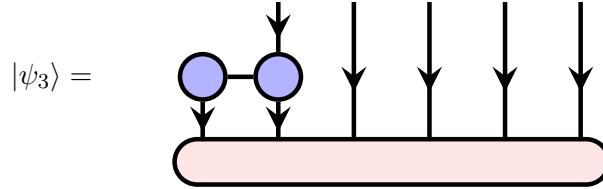
$$\begin{aligned} |E'_2\rangle &= \cos \theta_2 |00\rangle + \sin \theta_2 |11\rangle \\ |O'_2\rangle &= \cos \phi_2 |01\rangle + \sin \phi_2 |10\rangle \end{aligned}$$

for some angles θ_2 and ϕ_2 . These angles can be computed following the expression in (13) for the eigenvectors:

$$\theta_2 = \arctan\left(\frac{2s_e}{\sqrt{G_e^2 + 4s_e^2} + G_e}\right) \quad \text{and} \quad \phi_2 = \arctan\left(\frac{2s_o}{\sqrt{G_o^2 + 4s_o^2} + G_o}\right)$$

Here, $G_e = d_1 - d_2$ and $G_o = d_3 - d_4$ denote the gaps between the diagonal entries in each block. The angles should be thought of as measuring the deviation from perfect learning in step 2: if $f = 1$ then $G_e, G_o = 0$ and so $\theta_2 = \phi_2 = \pi/4$ which implies $|E'_2\rangle = |E_2\rangle$ and $|O'_2\rangle = |O_2\rangle$. In this case, step 2 has worked perfectly. Note that this is not an if-and-only-if scenario. Even if $f < 1$ then the reduced density may *still* have $|E_2\rangle$ and $|O_2\rangle$ as its eigenvectors. Indeed, this occurs whenever $G_e = G_o = 0$ and $s_e, s_o \neq 0$. In that case, the eigenvectors of ρ_2 are the desired parity vectors $|E_2\rangle, |O_2\rangle$, and the summarizer U_2 obtained is a true summarization tensor. But if G_e or G_o are both nonzero, then step 2 induces a summarization error, which we measure as the deviation of θ_2 and ϕ_2 from the desired $\pi/4$.

The analysis described here is repeated at each subsequent step $k = 3, \dots, N$, with minor adjustments to the combinatorics. So let us now describe the general schema. In the k th step of the training algorithm, each sample is cut after the k -th bit and viewed as a prefix-suffix pair $s = (a, b)$ where $a \in \Sigma^k$ and $b \in \Sigma^{N-k}$. Let $|\psi_k\rangle \in \mathbb{C}^{\Sigma^k} \otimes \mathbb{C}^{\Sigma^{N-k}}$ denote the sum of the samples after having completed step $k - 1$.



and let $\rho_k := \text{tr}_{\Sigma^{N-k}} |\psi_k\rangle\langle\psi_k|$ denote the reduced density on the prefix subsystem at step k . It is an operator on $B_{k-1} \otimes V_k$, where B_{k-1} is a 2-dimensional space which may be identified with the span of the eigenvectors associated to the two largest eigenvalues of ρ_{k-1} . As a matrix, ρ_k is a direct sum of 2×2 matrices,

$$(19) \quad \rho_k = \frac{1}{\text{tr}(\rho_k)} \begin{bmatrix} e0 & s_e & 0 & 0 \\ s_e & o1 & 0 & 0 \\ 0 & 0 & e1 & s_o \\ 0 & 0 & s_o & o0 \end{bmatrix}$$

We postpone a description of the entries until Section 5.2. But know that, as in the case when $k = 2$, the upper and lower blocks contains combinatorial information about prefixes of even and odd parity, respectively. As before, we are interested in the largest eigenvectors $|E'_k\rangle, |O'_k\rangle$ contributed by each block. They define the tensor U_k , which as a matrix has $|E'_k\rangle$ and $|O'_k\rangle$ along its rows, and can be understood inductively. The eigenvectors contain

combinatorial information from step k along with data from step $k - 1$. Let $|E'_1\rangle := |0\rangle$ and $|O'_1\rangle := |1\rangle$. Then for $k \geq 2$

$$\begin{aligned} |E'_k\rangle &= \cos \theta_k |E'_{k-1}\rangle \otimes |0\rangle + \sin \theta_k |O'_{k-1}\rangle \otimes |1\rangle \\ |O'_k\rangle &= \cos \phi_k |E'_{k-1}\rangle \otimes |1\rangle + \sin \phi_k |O'_{k-1}\rangle \otimes |0\rangle \end{aligned}$$

where

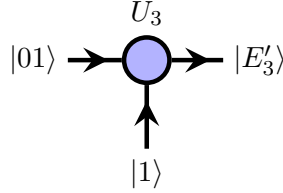
$$(20) \quad \theta_k = \arctan \left(\frac{2s_e}{\sqrt{G_e^2 + 4s_e^2} + G_e} \right) \quad \phi_k = \arctan \left(\frac{2s_o}{\sqrt{G_o^2 + 4s_o^2} + G_o} \right)$$

Again, the angles are a measurement of the error accrued in step k . Significantly, no error is accrued when the gaps $G_e := e0 - o1$ and $G_o := e1 - o0$ are zero and the off-diagonals s_e, s_o are non-zero, for then $\theta_k = \phi_k = \pi/4$. This outcome, or one close to it, is statistically favored for a wide range of training fractions.

As a matrix,

$$U_k = \begin{bmatrix} \cos \theta_k & \sin \theta_k & 0 & 0 \\ 0 & 0 & \cos \phi_k & \sin \phi_k \end{bmatrix}$$

and so U_k is akin to a map $B_{k-1} \otimes V_k \rightarrow B_k$ that combines previously summarized information from B_{k-1} with new information from V_k . It then summarizes the resulting data by projecting onto one of two orthogonal vectors, which may be identified with $|E'_k\rangle$ or $|O'_k\rangle$, in the new bond space B_k .



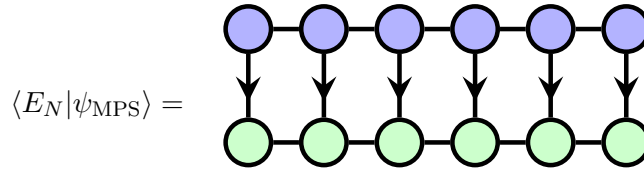
The true orientation of the arrows on U_k are down-left, rather than up-right. But the vector spaces in question are finite-dimensional, and our standard bases provide an isomorphism between a space and its dual. That is, no information is lost by momentarily adjusting the arrows for the purposes of sharing intuition.

In summary, this template provides a concrete handle on the tensors U_k that comprise the MPS factorization of $|\psi\rangle$.

5.1. High-level summary. We close by summarizing the high-level ideas present in this under-the-hood analysis. At the k th step of the training algorithm one obtains a 4×4 block diagonal reduced density matrix ρ_k . It is given in Equation (18) in the case when $k = 2$ and as in Equation (19) when $k > 2$. These matrices are obtained by tracing out the suffix subsystem from the projection $|\psi_k\rangle\langle\psi_k|$, where $|\psi_k\rangle$ is the sum of the samples in the training set after having completed step $k - 1$. Since $|\psi_k\rangle$ depends on the

error obtained in step $k - 1$, so does ρ_k . This error is defined by the angles θ_{k-1} and ϕ_{k-1} . As shown in Equation (20), these angles—and hence the error—are functions of the entries of the matrix representing ρ_{k-1} . So, the k th level density takes into account the errors accrued at each subsequent step as well as combinatorial information in the present step. A partial trace computation thus directly leads to the matrix representation for ρ_k given in Equation (19). Explicitly, the non-zero entries of the matrix are computed by Equations (23) and (24). With this, one has full knowledge of the matrix ρ_k and therefore of its eigenvectors $|E'_k\rangle, |O'_k\rangle$. Written in the computational basis, they are of the form shown in Equation (13). These two eigenvectors then assemble to form the rows of the tensor U_k , when viewed as a 2×4 matrix.

This analysis gives a thorough understanding of the error propagated at each step of the algorithm, as well as of the final MPS $|\psi_{\text{MPS}}\rangle$. To measure the algorithm's performance, we begin by evaluating the inner product of this vector with an MPS decomposition of the target vector $|E_N\rangle$.



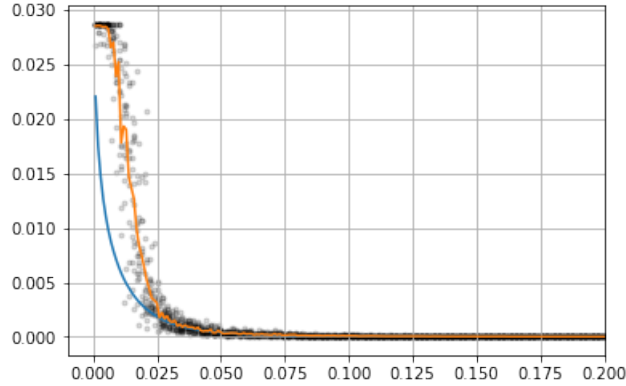
The k th tensor comprising the decomposition of $|E_N\rangle$ is equal to U_k when θ_k and ϕ_k are evaluated at $\pi/4$. The contraction thus results in a sum of products of $\cos \theta_k, \sin \theta_k, \cos \phi_k, \sin \phi_k$ for $k = 2, \dots, N$. More concretely, for each even bitstring $s \in E^N$ the inner product $\langle s | \psi_{\text{MPS}} \rangle$ is the square root of the probability of s . For now, we'll refer to it as the *weight* $w(s) := \langle s | \psi_{\text{MPS}} \rangle$ associated to the sample s . For each s , its weight $w(s)$ is a product of various $\cos \theta_k, \sin \theta_k, \cos \phi_k, \sin \phi_k$, the details of which are given in Section 5.2. The final overlap is then the sum

$$(21) \quad \langle E_N | \psi_{\text{MPS}} \rangle = \frac{1}{\sqrt{2^{N-1}}} \sum_{s \in E^N} w(s)$$

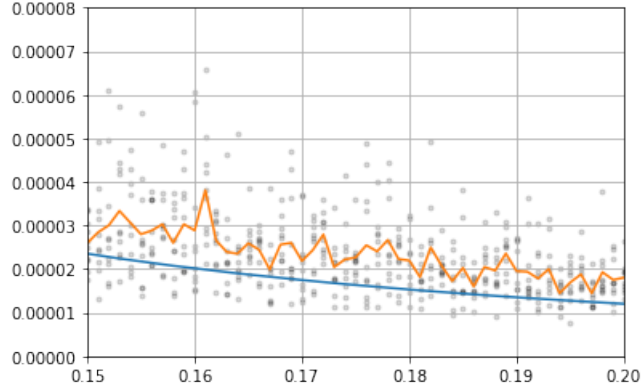
Now, suppose the training set consists of a fraction f of the entire population. The entries of the reduced densities in (19) are described combinatorially, as detailed in the next section. This makes it possible to make statistical estimates for gaps G_e and G_o and off-diagonal entries s_o and s_e in (20). Therefore, we can make statistical predictions for the angles θ_k and ϕ_k and hence for the tensors U_k comprising the trained MPS and the resulting generalization error. The results are plotted in Figure 4, where we use the Bhattacharya distance

$$(22) \quad - \frac{1}{\sqrt{2^{N-1}}} \ln \left(\sum_{s \in E^N} w(s) \right)$$

between the true population distribution and the one defined by either an experimentally trained MPS as a proxy for generalization error. The theoretical curve could, in principle, be improved by making more accurate statistical estimates for the combinatorics involved.



(A) The experimental average (orange) and theoretical prediction (blue).



(B) A closer look for $0.15 \leq f \leq 0.2$.

FIGURE 4. The experimental average (orange) and theoretical prediction (blue) of the weighted Bhattacharya distance between the probability distribution learned experimentally and the theoretical prediction for bit strings of length $N = 16$ and training set fractions of $0 < f \leq 0.2$.

5.2. Combinatorics of reduced densities. We now describe the entries of k th level reduced density in Equation (19). They depend on certain combinatorics in step k as well as error accumulated in the previous step. The latter has an inductive description. To start, observe that the parity of

a prefix $a \in \Sigma^k$ is determined by its last bit, together with the parity of its first $k - 1$ bits. The set Σ^k thus partitions into four sets:

$$E0 = \{a \in \Sigma^k : a = (e_{k-1}, 0) \text{ where } e_{k-1} \in E^{k-1}\}$$

$$O1 = \{a \in \Sigma^k : a = (o_{k-1}, 1) \text{ where } o_{k-1} \in O^{k-1}\}$$

$$E1 = \{a \in \Sigma^k : a = (e_{k-1}, 1) \text{ where } e_{k-1} \in E^{k-1}\}$$

$$O0 = \{a \in \Sigma^k : a = (o_{k-1}, 0) \text{ where } o_{k-1} \in O^{k-1}\}$$

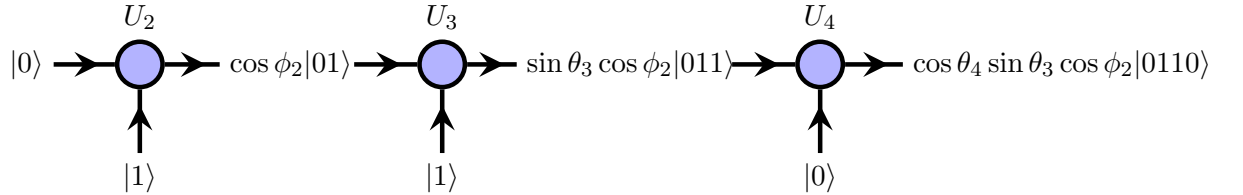
By viewing the training set as a bipartite graph, one has a visual understanding of these sets: $E0$ contains all prefixes of even parity whose last bit is 0; $O1$ contains all prefixes of even parity whose last bit is 1, and so on. In the example below with $k = 3$, we use color to distinguish each set.



As shown, each prefix also has a weight that records its contribution to the error accumulated in previous steps. Concretely, we assign to each prefix $a \in \Sigma^k$ a weight $w(a)$, which is a product of $k - 2$ terms. For $2 \leq i \leq k - 1$, the i th factor of $w(a)$ is defined to be

- $\cos \theta_i$ if the parity of the first $i - 1$ bits is even and the i th bit is 0
- $\sin \theta_i$ if the parity of the first $i - 1$ bits is odd and the i th bit is 1
- $\cos \phi_i$ if the parity of the first $i - 1$ bits is even and the i th bit is 1
- $\sin \phi_i$ if the parity of the first $i - 1$ bits is odd and the i th bit is 0

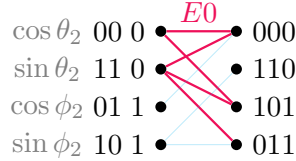
For example, if $k = 3$ then $w(011) = \cos \phi_2$. If $k = 5$ then $w(01101) = \cos \theta_4 \sin \theta_3 \cos \phi_2$. These weights are naturally associated to each tensor. For instance, recalling that each tensor U_k is akin to a summarizer, one sees $w(01101)$ in the following way:



We can now describe the entries of the reduced density defined in Equation (19). The first diagonal entry is

$$(23) \quad e0 = \sum_{\text{suffixes } b} \left(\sum_{\substack{a \in E0 \\ (a,b) \in T}} w(a) \right)^2$$

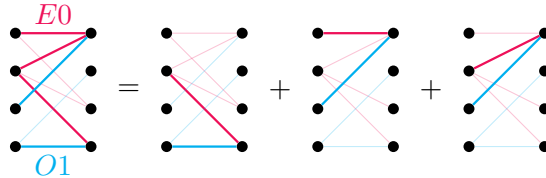
and the other diagonals are defined similarly. If perfect learning occurs then e_0 is, up to a normalizing constant, the sum of the squares of the degrees of each suffix, with respect to E_0 . For example, in the graph below e_0 is proportional to $2^2 + 2^2 + 1^2 = 9$.



In general, though, the summands will not be integers but rather products of weights. The off-diagonal entry in the even block of the reduced density is

$$(24) \quad s_e = \sum_{\text{suffixes } b} \left(\sum_{\substack{a \in E_0, a' \in O_1 \\ (a,b), (a',b) \in T}} w(a) \cdot w(a') \right)$$

When perfect learning occurs, s_e counts the number of paths of length 2, where now a path is comprised of one edge from E_0 and one edge from O_1 . For example, in the graph below $s_e = 3$.



In general, however, s_e will be a sum of products of weights. The expression for the off-diagonal s_o in the odd block is similar to that in Equation (24).

In summary, the theory behind the reduced densities and their eigenvectors gives us an exact understanding of the error propagated through each step of the training algorithm. We may then predict the Bhattacharya distance in (22) using statistical estimates of the expected combinatorics. This provides an accurate prediction based solely on the fraction f of training samples used and the length N of the sequences.

6. EXPERIMENTS

The training algorithm was written in the ITensor library [20]; the code is available on Github. For a fixed fraction $0 < f \leq 0.2$ we run the algorithm on ten different datasets, each containing $N_T = f2^{N-1}$ bitstrings of length $N = 16$. We then compare the average Bhattacharya distance in Equation (22) to the theoretical prediction. To handle the angles θ_k and ϕ_k in the theoretical model, we make a few simplifying assumptions about the expected behavior of the combinatorics.

First we assume $\theta = \phi_k$ for all k since the combinatorics of both blocks of the reduced densities ρ_k in (19) have similar behavior. We further assume the average angle θ is a function of the average off-diagonal s_e and the average diagonal gap G_e at the k th step, that is $\mathbb{E}[\theta_k(s_e, G_e)] = \theta_k(\mathbb{E}[s_e], \mathbb{E}[G_e])$ for all k . The expectation for s_e is experimentally determined to be independent of k , and dependent on the fraction f and bitstring length N alone: $\mathbb{E}[s_e] = f \cdot N_T/4$ for all k . We approximate the expected gap G_e at the k th step to be an experimentally determined function of f and the expected gap $G_2 = |d_1 - d_2|$ of the diagonal entries of the reduced density defined at step 2 of the algorithm. Understanding the expected behavior of G_2 is similar to understanding the statistics of a coin toss. On average, one expects to flip the same number of heads and tails and yet the expectation for their difference is non-zero. The distribution for G_2 is similar, but a little different:

$$\mathbb{E}[G_2] = \sum_{d_1} |2d_1 - r| \frac{\binom{n}{d_1} \binom{n}{r-d_1}}{\binom{2n}{r}}$$

where $r = d_1 + d_2 = N_T/2$ and $n = 2^{N-3}$ is the number of even parity bitstrings of length $N - 2$. The plots in Figure 4 compare the theoretical estimate against the experimental average.

7. CONCLUSION

Models based on tensor networks open interesting directions for machine learning research. Tensor networks can be viewed as a sequence of related linear maps, which by acting together on a very high-dimensional space allows the model to be arbitrarily expressive. The underlying linearity and powerful techniques from linear algebra allow us to pursue a training algorithm where we can look “under the hood” to understand each step and its consequences for the ability of our model to reconstruct a particular data set, the even-parity data set.

Our work also highlights the advantages of working in a probability formalism based on the 2-norm. This is the same formalism used to interpret the wavefunction in quantum mechanics; here we use it as a framework to treat classical data. Density matrices naturally arise as the 2-norm analogue of marginal probability distributions familiar from conventional 1-norm probability. Marginals still appear as the diagonal of the density matrix. Unlike marginals, the density matrices we use hold sufficient information to reconstruct the entire joint distribution. Our training algorithm can be summarized as estimating the density matrix from the training data, then reconstructing the joint distribution step-by-step from these density matrix estimates.

The theoretical predictions we obtained for the generative performance of the model agree well with the experimental results. Note that care is needed to compare these results, since the theoretical approach involves averaging over all possible training sets to produce a single typical weight MPS,

whereas the experiments produce a different weight MPS for each training-set sample. In the near future, we look forward to extending our approach to other measures of model performance and behavior, and certainly other data sets as well.

More ambitiously, we hope this work points the way to theoretically sound and robust predictions of machine learning model performance based on empirical summaries of real-world data. If such predictions can be obtained for training algorithms that also produce state-of-the art results, as tensor networks are starting to do, we anticipate this will continue to be an exciting program of research.

REFERENCES

- [1] Ulrich Schollwöck. The density-matrix renormalization group in the age of matrix product states. *Annals of Physics*, 326(1):96–192, 2011.
- [2] Steven R. White. Density matrix formulation for quantum renormalization groups. *Physical Review Letters*, 69(19):2863–2866, 1992.
- [3] E. Miles Stoudenmire and D. J. Schwab. Supervised learning with quantum-inspired tensor networks. *Advances in Neural Information Processing Systems (NIPS)*, 29:4799–4807, 2016.
- [4] M. M. Wolf D. Perez-Garcia, F. Verstraete and J. I. Cirac. Matrix product state representations. *Quantum Information and Computation*, 7:401–430, 2007.
- [5] E. Miles Stoudenmire. The tensor network, 2019. <http://tensornetwork.org>.
- [6] Glen Evenbly. Tensors.net, 2019. <https://www.tensors.net>.
- [7] Román Orús. A practical introduction to tensor networks: Matrix product states and projected entangled pair states. *Annals of Physics*, 349:117–158, 2014.
- [8] Alexander Novikov, Mikhail Trofimov, and Ivan Oseledets. Exponential machines. *arxiv:1605.03795*, 05 2016.
- [9] E Miles Stoudenmire. Learning relevant features of data with multi-scale tensor networks. *Quantum Science and Technology*, 3(3):034003, 2018.
- [10] Ivan Glasser, Nicola Pancotti, and J. Ignacio Cirac. Supervised learning with generalized tensor networks. *arxiv:1806.05964*, 06 2018.
- [11] Chu Guo, Zhanming Jie, Wei Lu, and Dario Poletti. Matrix product operators for sequence-to-sequence learning. *Phys. Rev. E*, 98:042114, Oct 2018.
- [12] Glen Evenbly. Number-state preserving tensor networks as classifiers for supervised learning. *arxiv:1905.06352*, 2019.
- [13] Ding Liu, Shi-Ju Ran, Peter Wittek, Cheng Peng, Raul Blázquez García, Gang Su, and Maciej Lewenstein. Machine learning by unitary tensor network of hierarchical tree structure. *New Journal of Physics*, 21(7):073059, jul 2019.
- [14] Stavros Efthymiou, Jack Hidary, and Stefan Leichenauer. TensorNetwork for machine learning. *arXiv:1906.06329*, 2019.
- [15] Zhao-Yu Han, Jun Wang, Heng Fan, Lei Wang, and Pan Zhang. Unsupervised generative modeling using matrix product states. *Phys. Rev. X*, 8:031012, Jul 2018.
- [16] Zhuan Li and Pan Zhang. Shortcut matrix product states and its applications. *arxiv:1812.05248*, 12 2018.
- [17] James Stokes and John Terilla. Probabilistic modeling with matrix product states. *arxiv:1902.06888*, 02 2019.
- [18] Song Cheng, Lei Wang, Tao Xiang, and Pan Zhang. Tree tensor networks for generative modeling. *Phys. Rev. B*, 99:155131, Apr 2019.

- [19] Ivan Glasser, Ryan Sweke, Nicola Pancotti, Jens Eisert, and J. Ignacio Cirac. Expressive power of tensor-network factorizations for probabilistic modeling, with applications from hidden Markov models to quantum machine learning. *arxiv:1907.03741*, 2019.
- [20] ITensor Library (version 3.0.0). <https://itensor.org>.

CUNY GRADUATE CENTER, NEW YORK, NY
E-mail address: `tbradley@gradcenter.cuny.edu`

FLATIRON INSTITUTE, NEW YORK, NY, A DIVISION OF THE SIMONS FOUNDATION
E-mail address: `mstoudenmire@flatironinstitute.org`

TUNNEL, NEW YORK, NY
E-mail address: `john@tunnel.tech`